

Application Analytical Method to Analysis of Spray Droplets

Ophir Nave

A Department of Mathematics, Jerusalem College of Technology (JCT), A Department of Mathematics Ben-Gurion University of the Negev

Abstract: The polydisperse fuel spray (droplets with different radii size) jet that discharging into a hot gas is study in this paper. The dimensionless governing equations (a PDE system) of the physical model include a gas-phase equations and liquid-phase equations. The analysis of the model is based on the well-known semi-analytical method the homotopy analysis method (HAM). In the frame of the HAM the so-called convergence-control parameter is an artificial parameter of the model which provides a convenient way to guarantee the convergence of approximation series of the solutions.

Keywords: Droplet combustion, homotopy analysis method (HAM), Fuel Spray

I. Introduction

The analysis of a group vaporization of a polydisperse fuel-spray jet discharging into a hot co-flowing gaseous stream is very applicable in engineering science. [1]-[2]. In most cases, the investigation of these models based on asymptotic analysis and numerical simulations. In very few cases for very specific models researchers can applied an analytical methods. When one applied a numerical method, the researcher can include a lot of physical phenomena and even he should not neglect any expression in the model. Applying an analytical method, one should simplify the model in order to get an analytical expressions, on the other hand, analytical and asymptotic method are better suit for isolating the most important physical effects, thereby increasing understanding of the underlying physical significantly. In addition, analytical and asymptotic methods often can yield an expressions and formulas that are readily applied to calculate quantities of interest in engineering applications [3].

In this paper we investigated the model that includes a polydisperse fuel spray jet discharging with high Reynolds number into a surrounding hot co-flow. This model extends the model present in [4]. In order to understand this model from physical point of view, one should identify the key controlling parameters and study their influence on the spray structure. For example, the parameter that representing the mass of liquid fuel per unit mass of gas in the spray stream has been identify in the above model and assumed to be in order of 1 i.e. $\alpha_c \approx O(1)$.

One of the analytical-numerical method that we applied in this paper is the well-known the homotopy analysis method [5]. This method do not involve perturbation series in powers of physical parameters, and the convergence of approximate is controlled by an artificial parameter called \hbar which do not exists in the original physical model. When one apply the HAM, then this artificial parameter is fixed at the end of calculations according to some criterion such as the principle of minimal sensitivity (PMS), which requires the approximants have the least dependence on these parameters over perturbation techniques.

The biggest advantage of the HAM method, which is different from all other analytical methods, is that it provides us with a simple way to adjust and control the convergence region of solution series by choosing proper values of auxiliary parameter \hbar , auxiliary function H and auxiliary linear operator L (for more details [6]).

II. Conservation Equations

2.1 Characteristic time scales

In general when dealing with the spray vaporization process there are three characteristic time scales that are involved in this process: the first one is the diffusion time across the jet due to the comparison the convection and transverse diffusion in the gas-phase conservation equation $t_D = R^2 / D_{T_j}$ where $D_{T_j} = \kappa / (\rho_j \cdot c_p)$, the second is the droplet lifetime which is characterizes the vaporization of each individual droplet and given by $t_{r_d} = (\rho_l \cdot r_{d_j}^2) / (3\rho_j \cdot D_{T_j})$ and the third one is the spray-interaction time which include the effect of spray vaporization on the density, velocity, temperature, and fuel-vapor evolution in the jet and given by $t_s = (4\pi r_{d_j} n_{d_j} D_{T_j})^{-1}$, this time scale corresponds to the characteristic time required for droplet vaporization to change appreciably, by a relative of order unity-the value of the gas density in the jet.

2.2 Controlling parameters

In this section we present two controlling parameters that are related to the time scales. The first one is the characteristic time ratio $\alpha_c = t_{r_d} / t_s$ which is measuring the dilution of the spray, and corresponds to the spray configuration with characteristic values of the average distance between neighboring droplets and given by $\alpha_c = (4\pi/3)r_{d_j}^3 n_{d_j} \rho_l / \rho_j$.

The second controlling parameter is the ratio of the characteristic time of jet evolution due to the spray vaporization t_s to the diffusion time t_D and given by $\varepsilon = (4\pi r_{d_j} n_{d_j} R^2)^{-1}$.

This parameter is useful when one applying an asymptotic analysis of droplets cloud vaporization because its value is small and causing vaporization to occur in a sheath or vaporization front that separates the spray, in saturated equilibrium, from the surrounding droplet-free hot gas, with the flame standing outside the spray in combustion configurations.

2.3 The physical model

Our non-dimensional model take into account a different droplet radii size i.e., polydisperse spray in a continuous way by using probability density function. The characteristic diffusion time will be used to construct scales for the stream-wise length, $U_j t_D$, and for the gas and droplet radial velocities, $R/t_D = D_{T_j} / R$. The radial distance will be scaled with R , whereas the droplet and the gas axial velocity components, the droplet radius and the number density, and the gas temperature and density will be scaled with their values at the spray exit. Under these assumptions the governing equation are as follows [4]:

Gas-phase equations

$$\partial_x(\rho u) + \frac{1}{r} \partial_r(\rho r v) = \frac{1}{\epsilon} \ln \left(1 + \frac{T-1}{\beta} \right) \cdot \int_0^\infty P(r_d) r_d dr_d, \quad (2.1)$$

$$\begin{aligned} \partial_x(\rho u^2) + \frac{1}{r} \partial_r(\rho r v u - P r(r \partial_r u)) &= \frac{1}{\epsilon} \ln \left(1 + \frac{T-1}{\beta} \right) \cdot \int_0^\infty P(r_d) r_d u dr_d \\ &+ \frac{3Pr}{2\epsilon} \cdot \int_0^\infty (u_d - u) P(r_d) r_d dr_d, \end{aligned} \quad (2.2)$$

$$\partial_x(\rho u T) + \frac{1}{r} \partial_r(\rho r v T - (r \partial_r T)) = -\frac{\beta-1}{\epsilon} \ln \left(1 + \frac{T-1}{\beta} \right) \cdot \int_0^\infty P(r_d) r_d dr_d, \quad (2.3)$$

$$\partial_x(\rho u Y) + \frac{1}{r} \partial_r \left(\rho r v Y - \frac{1}{L} (r \partial_r Y) \right) = \frac{1}{\epsilon} \ln \left(1 + \frac{T-1}{\beta} \right) \cdot \int_0^\infty P(r_d) r_d dr_d, \quad (2.4)$$

Liquid-phase equations

$$\begin{aligned} \partial_x \left(\int_0^\infty P(r_d) r_d^3 u_d dr_d \right) + \frac{1}{r} \partial_r \left(r \cdot \int_0^\infty P(r_d) r_d^3 v_d dr_d \right) \\ = - \frac{\ln \left(1 + \frac{T-1}{\beta} \right)}{\epsilon \alpha_c} \cdot \int_0^\infty P(r_d) r_d dr_d, \end{aligned} \quad (2.5)$$

$$\begin{aligned} \partial_x \left(\int_0^\infty P(r_d) r_d^3 u_d dr_d \right) + \partial_r \left(\int_0^\infty P(r_d) r_d^3 v_d dr_d \right) \\ = - \frac{\ln \left(1 + \frac{T-1}{\beta} \right)}{\epsilon \alpha_c} \cdot \int_0^\infty P(r_d) r_d dr_d, \end{aligned} \quad (2.6)$$

$$\begin{aligned} \partial_x \left(\int_0^\infty P(r_d) r_d^3 u_d w_d dr_d \right) + \partial_r \left(\int_0^\infty P(r_d) r_d^3 v_d w_d dr_d \right) \\ = - \frac{\ln \left(1 + \frac{T-1}{\beta} \right)}{\epsilon \alpha_c} \cdot \int_0^\infty P(r_d) r_d w_d dr_d \\ + \frac{3Pr}{2\epsilon \alpha_c} \cdot \int_0^\infty P(r_d) r_d (w - w_d) dr_d, \end{aligned} \quad (2.7)$$

where $w = u - v$, $w_d = u_d - v_d$.

The initial and boundary conditions of the problem are

$$\begin{aligned} \text{at } x = 0 : \text{ for } r < 1 : u = T = P = R = u_d = 1, Y = Y_j, v_d = 0, \\ \text{at } x = 0 : \text{ for } r > 1 : u = u_c, T = T_c, Y = 0, \\ \text{at } x > 0 : \text{ for } r = 1 : v = \partial_r u = \partial_r T = \partial_r Y = 0, \\ \text{at } x > 0 : \text{ for } r \rightarrow \infty : u = u_c, T = T_c, Y = 0. \end{aligned} \quad (2.8)$$

III. Analysis And Numerical Results

One of the analytical-numerical method that we applied in this paper is the well-known the homotopy analysis method. In general, perturbation methods are widely used to investigate physical systems that can be exactly solved, but these systems need to contain small perturbations parameters in order to apply different perturbation methods. In contrast to the classical perturbation method, the HAM is always valid no matter whether there exist small physical parameters or not in the system. The HAM contains the auxiliary parameter so-called the artificial parameter \hbar [5]. This means that this method do not involve perturbation series in powers of physical parameters, and the convergence of approximate is controlled by \hbar which do not exists in the original physical model. The biggest advantage of the HAM method, which is different from all other analytical methods, is that it provides us with a simple way to adjust and control the convergence region of solution series by choosing proper values of auxiliary parameter \hbar , auxiliary function H and auxiliary linear operator L (for more information about the symbols please refer to [6]). A comparison with experimental data enables one to validate the new model and the validity of the HAM method.

3.1 The homotopy analysis method procedure

Consider the following differential equation:

$$N(u(\vec{r}, t)) = 0. \quad (3.1)$$

where N is a nonlinear operator, r is a vector of spatial variables, t denotes time and u is an unknown function.

3.1.1 Zero order deformation of HAM

By means of generalizing the traditional concept of homotopy, Liao [7] constructs the so-called zero-order deformation equation:

$$(1 - p)\ell [\Phi(\vec{r}, t; p) - u_0(\vec{r}, t)] = \hbar H(\vec{r}, t)N(\Phi(\vec{r}, t; p)), \quad (3.2)$$

where \hbar is a non-zero auxiliary parameter, H is an auxiliary function, ℓ is an auxiliary linear operator, $u_0(\cdot)$ is an initial guess of $u(\cdot)$, Φ is a unknown function. The degree of freedom is to choose the initial guess, the auxiliary linear operator, the auxiliary parameter, and the auxiliary function H . Expanding Φ to a power series with respect to the embedding parameter p , one has

$$\Phi(\vec{r}, t; p) = u_0(\vec{r}, t) + \sum_{n=1}^{\infty} u_n(\vec{r}, t)p^n, \quad (3.3)$$

Where

$$u_n(\vec{r}, t) = \frac{1}{n!} \left. \frac{\partial^n \Phi(\vec{r}, t; p)}{\partial p^n} \right|_{p=0}. \quad (3.4)$$

If the auxiliary linear operator, the initial guess, the auxiliary parameter, and the auxiliary function are so properly chosen that the above series converges at $p = 1$, one has

$$\Phi(\vec{r}, t; p) = u_0(\vec{r}, t) + \sum_{n=1}^{\infty} u_n(\vec{r}, t), \quad (3.5)$$

which must be one of the solutions of the original nonlinear equation, as proved in [7].

3.1.2 mth-order deformation

Define the vector:

$$\vec{u}_n(\vec{r}, t) = \{u_0(\vec{r}, t), u_1(\vec{r}, t), \dots, u_n(\vec{r}, t)\}. \quad (3.6)$$

Differentiating Equation (3.2) m -times with respect to the embedding parameter p and then setting $p = 0$ and finally dividing the terms by $m!$, we obtain the m -order deformation equation in the form of:

$$\ell[u_m(\vec{r}, t) - \chi_m u_{m-1}(\vec{r}, t)] = \hbar H(\vec{r}, t)R_m(u_{m-1}(\vec{r}, t)), \quad (3.7)$$

where,

$$R_m(u_{m-1}(\vec{r}, t)) = \frac{1}{(m-1)!} \left. \frac{\partial^{m-1} N(\Phi(\vec{r}, t; p))}{\partial p^{m-1}} \right|_{p=0}, \quad (3.8)$$

and χ_m is the unit step function. Applying the inverse operator ℓ^{-1} on both side of Equation (3.7), we get

$$u_m(\vec{r}, t) = \chi_m u_{m-1}(\vec{r}, t) + \hbar \ell^{-1}[H(\vec{r}, t)R_m(u_{m-1}(\vec{r}, t))]. \quad (3.9)$$

In this way, it is easy to obtain u_m for $m > 1$, at m -order and finally get the solution as:

$$u(\vec{r}, t) = \sum_{n=0}^m u_n(\vec{r}, t). \quad (3.10)$$

when $M \rightarrow \infty$ we get an accurate approximation of the original equation (3.1). For the convergence of the above method we refer the reader to [7]. If equation (3.1) admits unique solution, then this method will produce the unique solution. If equation (3.1) does not possess unique solution, the HAM will give a solution among many other (possible) solutions.

Figures 1 – 6 correspond to numerical simulations and homotopy analysis method. Figure 1 shows the solutions profiles of the temperature obtained by numerical simulation. As can be seen from this figure, when the axial location is far the temperature decrease faster, i.e., near to the beginning of the process. In addition the width of the sprays is increased as the axial location increased. The analysis of the solutions profiles for temperature when we implemented the homotopy analysis method (Figure 2) is similar. Here the temperature decrease faster when axial location is far in comparing to the numerical simulations but the spray width wider.

Figures 3 – 4 shows the solutions profiles of the radius obtained by numerical simulation and HAM method correspondingly. The solutions profiles of the radius, which shows the decrease of the radius, are compatible with the solutions profiles of the temperature for both of the methods. For example, the temperature in the Sub-graph 2 in Figure 1 is higher at ≈ 1.1 . This result is consistent with the sub-graph 2 in Figure 3, i.e., the radius decrease to zero at ≈ 1.1 . Adjusting these results also apply to the rest of sub-graphs. Finally the droplets is completely consumed at a finite distance from the injector at $x \approx 2.1$, so that farther downstream the spray boundary is defined as the location where $r = 0$ corresponding to vaporizing droplets located initially within the jet away from the injector edge.

Figures 5 – 6 shows the solutions profiles of the mass fraction obtained by numerical simulation and HAM method for different values of α_c and ε , including dilute ($\alpha_c = 1$) and dense ($\alpha_c = 25$) sprays correspondingly. As shown if these figure the vaporization occurs in a distributed manner for $\varepsilon = 1$. In particular, although the vaporization is more pronounced at the edge of the spray, non-negligible vaporization of the droplets located along the axis can be seen already at $x \approx 0.4$. As results, the fuel mass fraction increases from its initial value $Y_j = 0.2$, giving profiles that peak at the axis. In addition the this analysis is that the heat transfer from the hot coflow increases the temperature within the spray to values significantly larger than the boiling point temperature $T = 1$. Figure 7 shows the relative error between the numerical simulations and the HAM analysis. Figure 8 shows the valid region of the so-called the convergence-control parameter for different m-order deformation when applying the homotopy analysis method.

IV. Conclusions

Many problems which arise in applied mathematics are highly non-linear and thus can be difficult or impossible to solve analytically. The Homotopy Analysis Method (HAM) is a semi-analytical technique used to solve differential equations, in particular non-linear and partial. Different from all other analytical methods, it provides us with a simple way to adjust and control the convergence region of solution series by choosing proper values of the different quantities in the HAM method. As our results shown, we have great freedom to choose the auxiliary parameter, the so-called the convergence-control parameter, the auxiliary function H, the auxiliary linear operator L and the initial guesses. In addition, the HAM was shown to be simple, yet powerful analytic-numeric scheme for solving various nonlinear problems. Numerical computation has been done by Matlab software package.

References

- [1]. Marley S.K., Lyons K.M., Watson K.A., Leading-edge reaction zones in lifted-jet gas and spray flames, *Flow Turbulence and Combustion*, 72(1):29- 47, (2004).
- [2]. Hamelnick L., Greenberg J.B., A simple model of multiple spray flames and their interaction, 49th AIAA Aerospace Sciences Meeting including the New Horizons Forum and Aerospace Exposition, 2011, Orlando, Florida.
- [3]. Nave O., Bykov V. Gol'dshtein V., A probabilistic model of thermal explosion in polydisperse fuel spray, *Applied Mathematics and Computation*, 217(6):26982709, (2010).
- [4]. Urzay J., Mart'inez-Ruiz D., Sanchez A.L., Lianan M. A., and Williams, F.A., Flamelet structures in spray ignition. *Nasa-Stanford Annual Research Briefs*, 107-122 (2013).
- [5]. Shuijun L., On the homotopy analysis method for nonlinear problems, *Applied Mathematics and Computation*, 147:499-513 (2004).
- [6]. Shuijun L., Homotopy analysis method: A new analytic method for non-linear problems, *Applied Mathematics and Mechanics*, 19:957-962 (1998).
- [7]. Shuijun L., *Beyond Perturbation: Introduction to the Homotopy Analysis Method (Modern Mechanics and Mathematics)*, CHAPMAN & HALL/CRC, (2003).

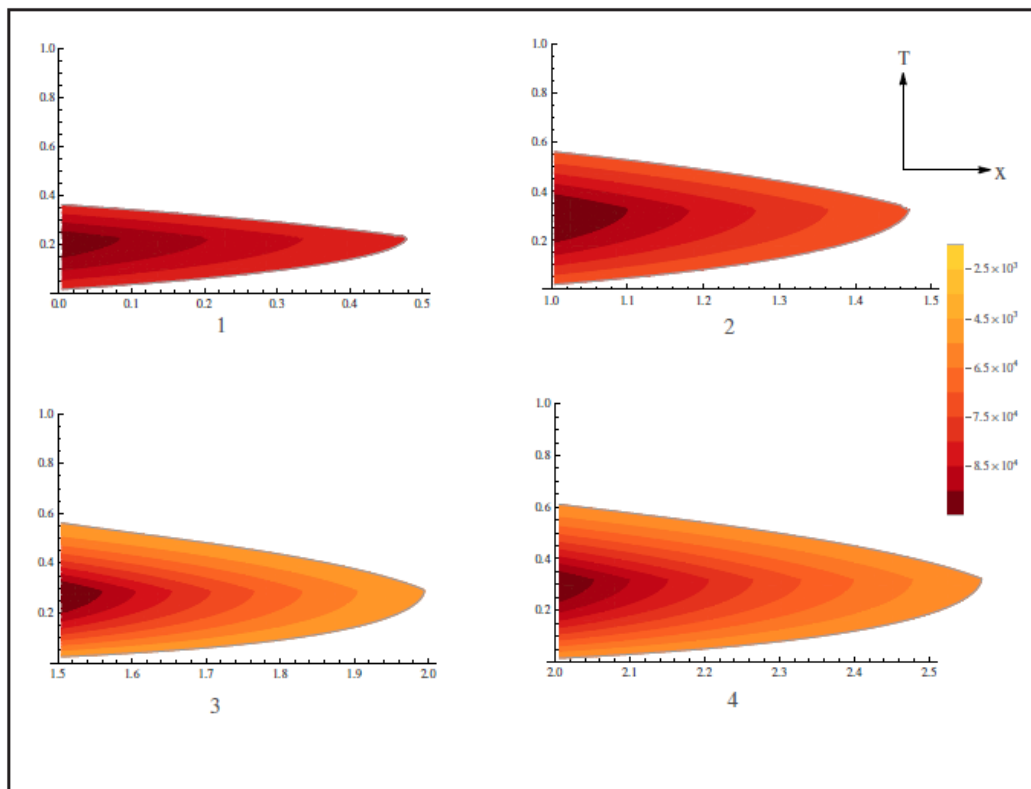


Figure 1: Solutions profiles of the temperature across the vaporizing jet obtained by numerical simulation for $u_c = 1, L = 1, Y_j = 0.2, Pr = 0.7, \beta = 0.36, T_c = 2.15, \alpha_c = 1, \varepsilon = 1$.

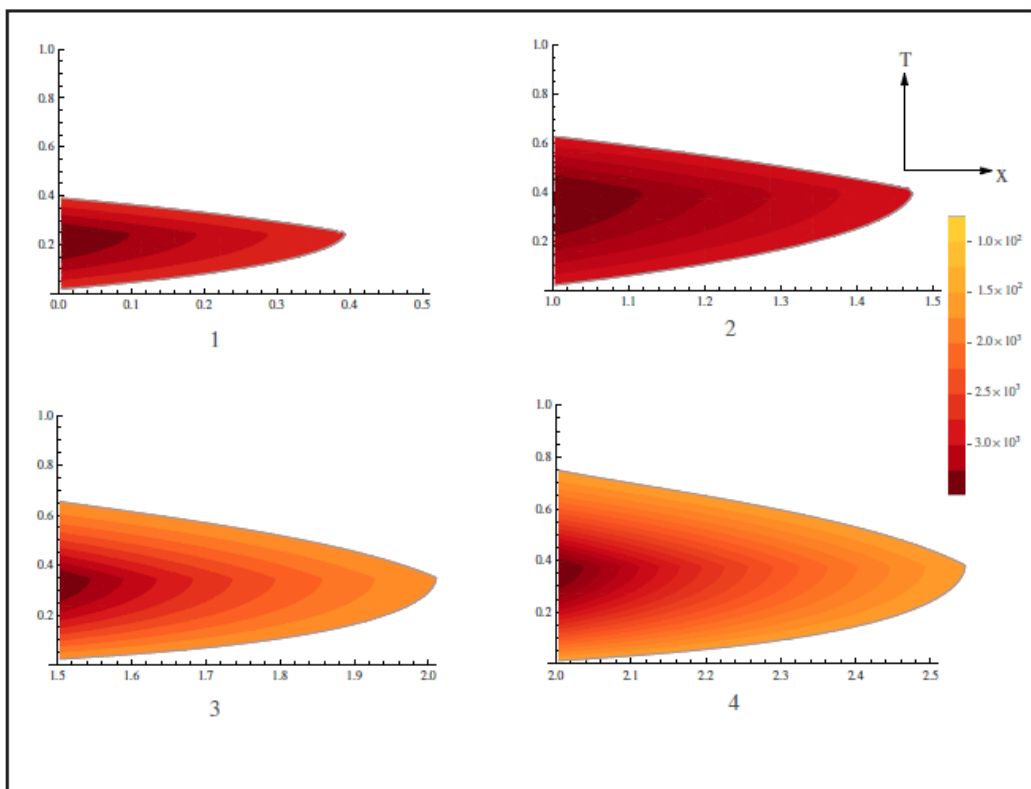


Figure 2: Solutions profiles of the temperature across the vaporizing jet obtained by applying the homotopy analysis method for 50th-order for $u_c = 1, L = 1, Y_j = 0.2, Pr = 0.7, \beta = 0.36, T_c = 2.15, \alpha_c = 1, \varepsilon = 1$.

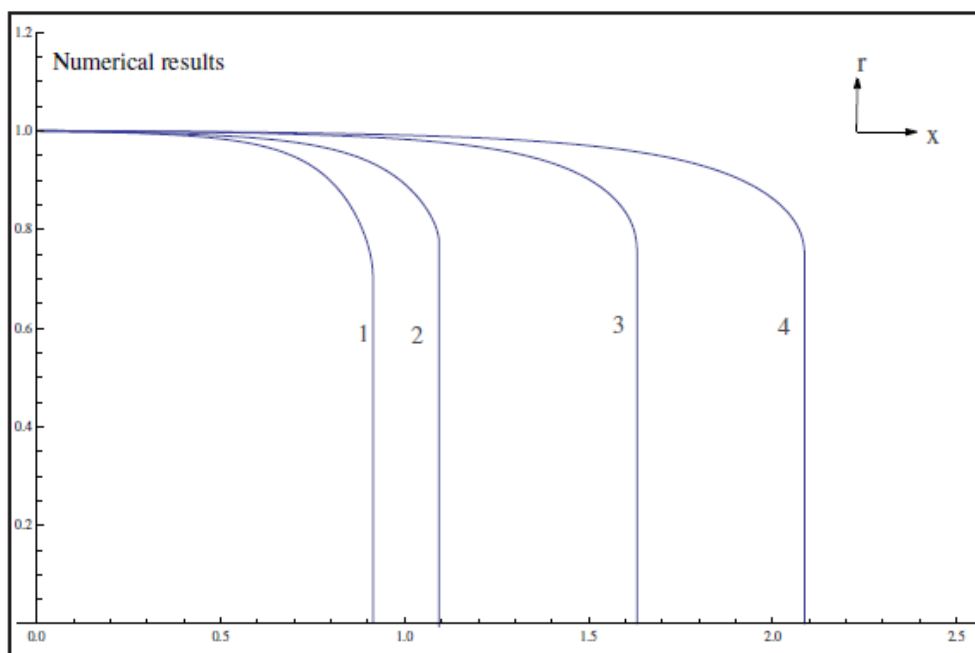


Figure 3: Solutions profiles of the radius across the vaporizing jet obtained by numerical simulation and compatible with Figure 4.1 for $u_c = 1, L = 1, Y_j = 0.2, Pr = 0.7, \beta = 0.36, T_c = 2.15, \alpha_c = 1, \varepsilon = 1$.

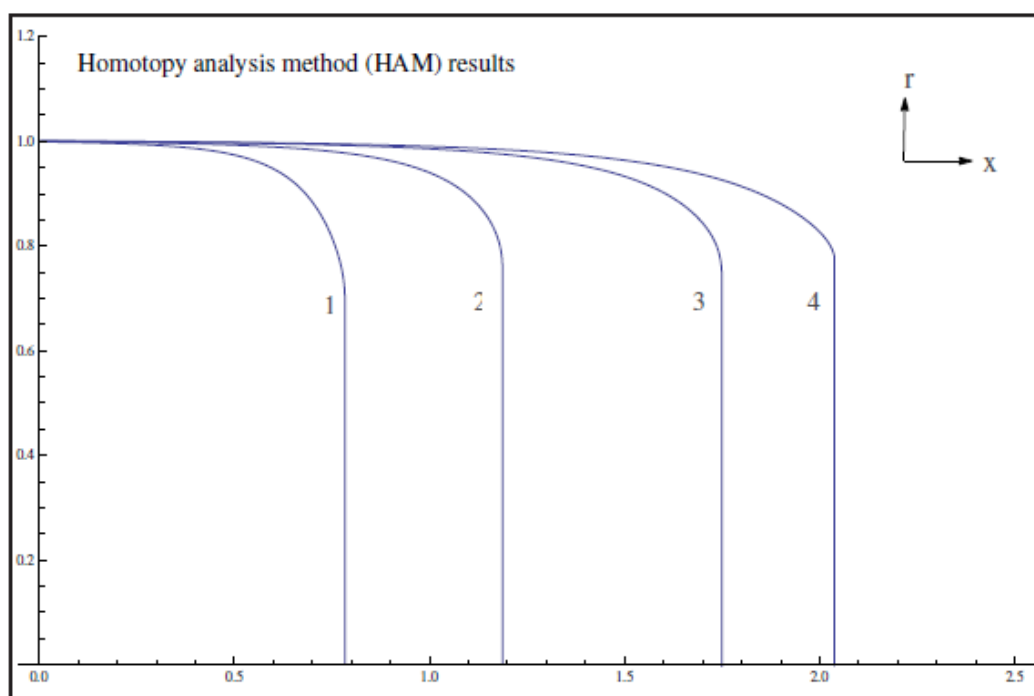


Figure 4: Solutions profiles of the radius across the vaporizing jet obtained by applying the homotopy analysis method and compatible with Figure 4.2 for $u_c = 1, L = 1, Y_j = 0.2, Pr = 0.7, \beta = 0.36, T_c = 2.15, \alpha_c = 1, \varepsilon = 1$.

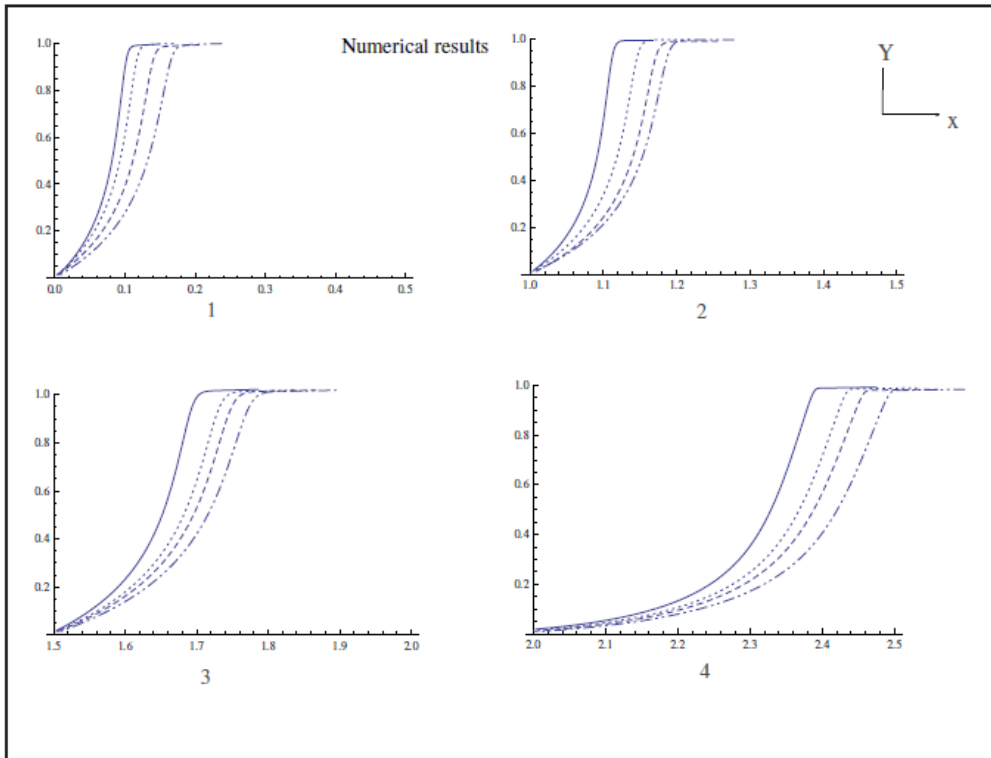


Figure 5: Solutions profiles of the mass fraction across the vaporizing jet obtained by numerical simulation for different values of α_c and ϵ , including dilute ($\alpha_c = 1$) and dense ($\alpha_c = 25$) sprays. The following parameters are used: $u_c = 1, L = 1, Y_j = 0.2, Pr = 0.7, \beta = 0.36, T_c = 2.15, \alpha_c = 1, \epsilon = 1$.

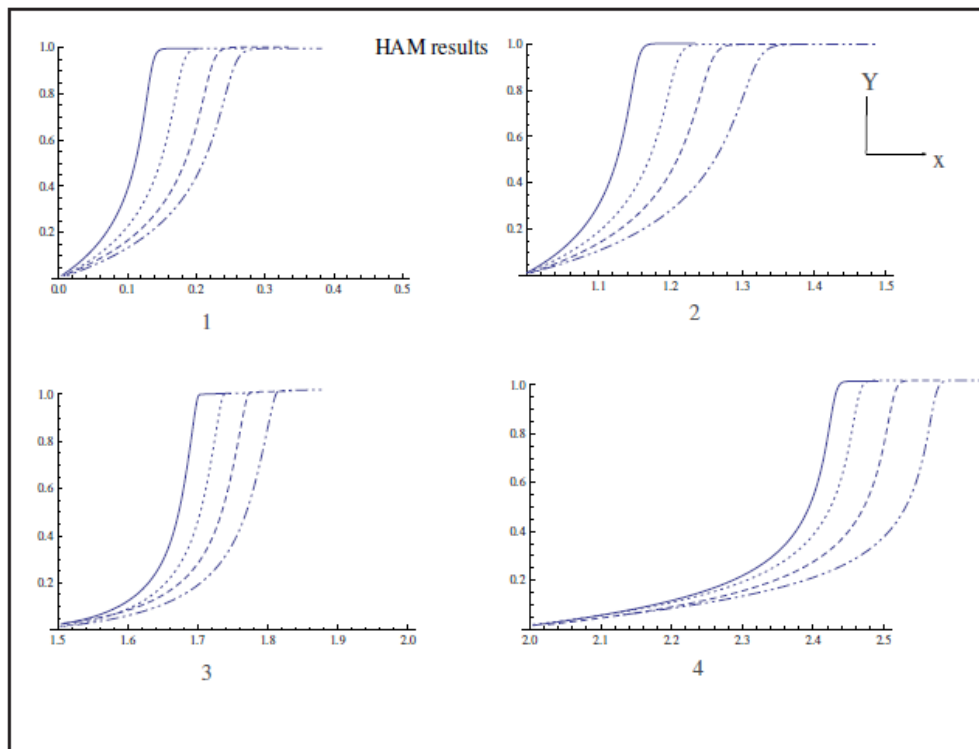


Figure 6: Solutions profiles of the mass fraction across the vaporizing jet obtained by applying the homotopy analysis method for different values of α_c and ϵ , including dilute ($\alpha_c = 1$) and dense ($\alpha_c = 25$) sprays. The following parameters are used: $u_c = 1, L = 1, Y_j = 0.2, Pr = 0.7, \beta = 0.36, T_c = 2.15, \alpha_c = 1, \epsilon = 1$.

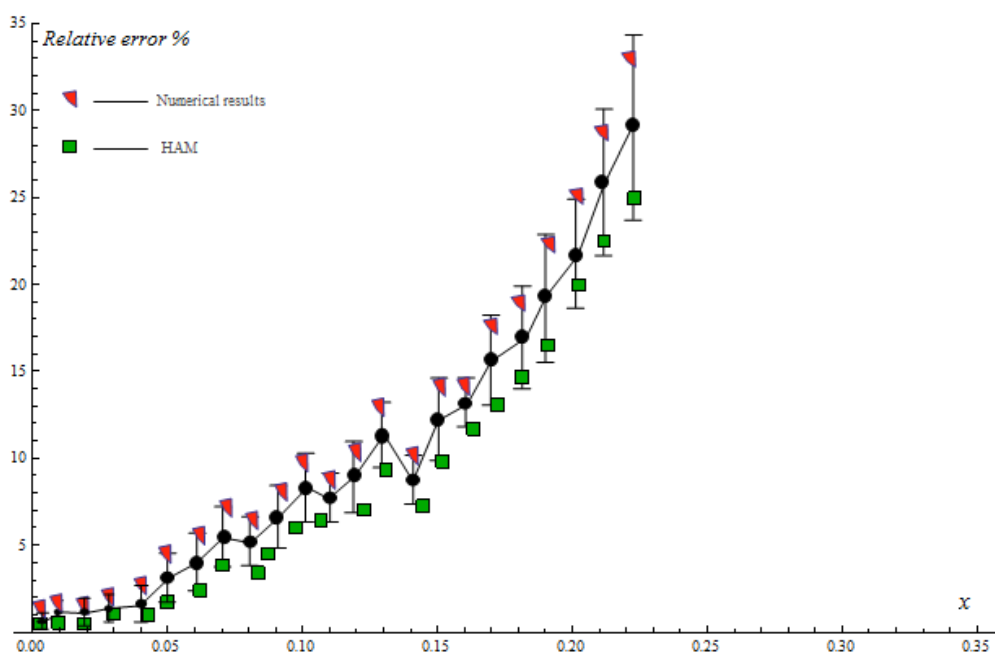


Figure 7: The relative error between numerical results and HAM analysis

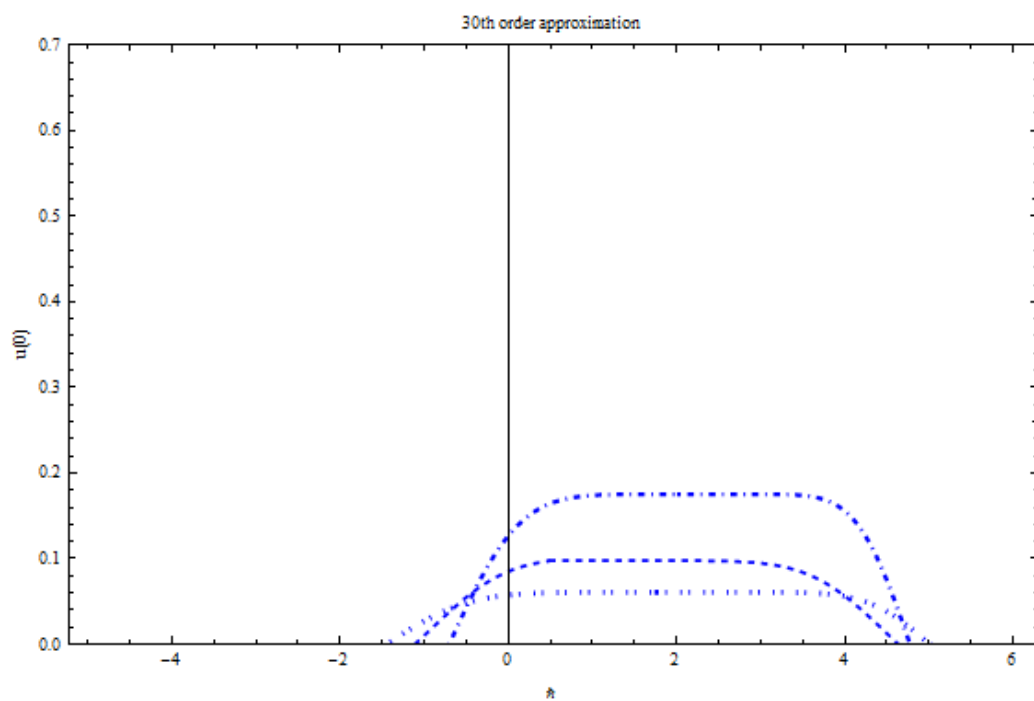


Figure 8: The valid region of the convergence control parameter.